Annealing behavior of cryogenically-rolled Cu-30Zn brass

T. Konkova[a], S. Mironov[a,b], A. Korznikov[a,c], G. Korznikova[a], M.M. Myshlyaev[d], S.L. Semiatin

[a]Institute for Metals Superplasticity Problems, Russian Academy of Science, Ufa 450001, Russia
[b]Institute for Metals Superplasticity Problems, Russian Academy of Science, Ufa 450001, Russia; and Department of Materials Processing, Graduate School of Engineering, Tohoku University, Sendai 980-8579, Japan
[c]National Research Tomsk State University, Tomsk 634050, Russia
[d]Baikov Institute of Metallurgy and Material Science, Russian Academy of Science, Moscow 119991, Russia; and Institute of Solid State Physics, Russian Academy of Sciences, Chernogolovka, Moscow oblast 142432, Russia
[e]Air Force Research Laboratory, Materials and Manufacturing Directorate, AFRL/RXCM, Wright-Patterson AFB, Ohio 45433-7817, USA

The static-annealing behavior of cryogenically-rolled Cu-30Zn brass over a wide range of temperature (100-900 C) was established. Between 300 and 400 C, microstructure and texture evolution were dominated by discontinuous recrystallization. At temperatures of 500 C and higher, annealing was interpreted in terms of normal grain growth. The recrystallized microstructure developed at 400 C was ultrafine with a mean grain size of 0.8 μm, fraction of high-angle boundaries of 90 pct., and a weak crystallographic texture.

Keywords:

Metals and alloys
Nanostructured materials
Nanofabrications
Microstructure
Scanning electron microscopy

1. Introduction

Large deformation at cryogenic temperatures is sometimes considered as a promising and cost-effective method for producing bulk ultrafine-grain materials [1-9]. This approach is believed to be particularly effective for materials prone to mechanical twinning and/or shear banding. However, recent studies of cryo-rolled Cu-30Zn brass have shown that the microstructure so produced may be extremely inhomogeneous, consisting of mm-scale remnants of original grains intermixed with ultrafine-grain domains [8,9]. This observation has been attributed to the relatively-low twinning-to-slip Schmid-factor ratio for grains having crystallographic orientations close to Brass {110}<112> and Goss {110}<100> [8,9]. Since these two orientations are well known to be very stable during rolling of low-stacking-fault-energy (SFE) cubic alloys [10], the volume fraction of the coarse-grain remnants may be relatively large.

One possible way to overcome this problem (and thus develop a reasonably homogenous ultrafine-grain structure) may be recrystallization annealing following cryogenic rolling. The energy stored in cryo-rolled, low-SFE materials is believed to be large, and hence the size of the recrystallization nuclei may be within the ultrafine grain range ($\leq$ 1 μm). Moreover, these alloys are prone to the formation of annealing twins, a factor which could promote additional grain refinement during final heat treatment. To establish the veracity of such hypotheses, the broad aspects of the annealing behavior of cryo-rolled Cu-30Zn brass were evaluated in this work.

2. Material and experimental procedures

The program material comprised Cu-30Zn with a measured composition (in wt.%) of 29.5 Zn, 0.5 Pb, and balance Cu. The alloy was produced by the casting an ingot, which was broken down via10% cold rolling followed by a 30-min anneal at 800 C. Sections of this material were then cryogenically rolled to 90-pct. overall thickness reduction (true strain ≈ - 2.3) using multiple passes of ~10 pct. each. In order to provide cryogenic-deformation conditions, the rolling perform and work rolls were soaked in liquid nitrogen prior to each pass and held for 20 min; immediately after each pass, the workpiece was re-inserted into liquid nitrogen. The typical flat-rolling convention was adopted in this work; i.e., the rolling, long-transverse, and thickness/normal directions were denoted as RD, TD, and ND, respectively.

To investigate the subsequent annealing behavior of the cryorolled material, samples were furnace annealed over a range of temperatures from 100 C (0.30 T_m, where T_m is the melting point) to 900 C (0.95 T_m) for 1 h. In all cases, annealing was conducted in air. Following heat treatment, each specimen was water quenched. To preserve the microstructures developed during each thermomechanical treatment, the cryo-rolled as well as annealed samples were stored in a freezer at ~20 C prior to examination.

To provide in-depth insight into the microstructures and crystallographic textures so developed, characterization was performed by electron back-scatter diffraction (EBSD) technique. In all cases, the mid-thickness rolling plane (containing the RD and TD) was examined. For this purpose, samples were prepared using conventional metallographic techniques followed by long-term (24 h) vibratory polishing with a colloidal-silica suspension. EBSD analysis was conducted using JSM-7800F and Hitachi S-4300SE field emission-gun scanning-electron microscopes each equipped with a TSL EDAX OIM™ EBSD system. To determine the microstructure at different length scales, several EBSD maps were acquired from each sample using different scan-step sizes ranging from 0.05 to 5 μm. To improve the reliability of the EBSD data, small grains comprising three or fewer pixels were automatically removed from the maps using the grain-dilation option in the TSL software. Furthermore, to eliminate spurious boundaries caused by orientation noise, a lower limit boundary-misorientation cutoff of 2^o was used. A 15^o criterion was employed to differentiate low-angle boundaries (LABs) and high-angle boundaries (HABs). Grain size was quantified by the determination of the area of each grain and the calculation of its circle-equivalent diameter [11].

To obtain a broader view of microstructure evolution, the Vickers microhardness was also measured on each sample using a load of 100 g for 10 s. For this purpose, 25 measurements were made in each case to obtain an average value.

3. Results

3.1. Hardness data and microstructure evolution

The effect of annealing temperature on microhardness is shown in Fig. 1. Several different temperature regimes were observed in the data. For temperatures of 100-200 C (0.30-0.38 T_m), relatively-high hardness values were observed. At 300 C (0.46 T_m), an abrupt decrease in hardness took place followed by a more gradual decrease which appeared to saturate at 800 C (0.87 T_m).

A number of details of microstructure evolution were revealed by EBSD maps for the cryo-rolled and annealed specimens; typical examples are shown in Fig. 2. In these maps, LABs, HABs, and Σ3 twin boundaries (within a 5° tolerance) are depicted by red, black, and gray lines, respectively. The overall statistics from the grainsize and misorientation measurements are given in Fig. 3.

The microstructure of the as-cryo-rolled sample (Fig. 2a) was markedly inhomogeneous and could be described in terms of remnants of coarse original grains with poorly-developed substructure and ultrafine-grain domains. The latter regions consisted of shear bands, mechanical twins, and a dense LAB substructure. The mean grain size in the ultrafine-grain areas was ~0.2 μm.

In the temperature range of 100-200 C (0.30-0.38 Tm), the grain structure was found to be relatively stable, showing no significant changes in morphology, grain size, or misorientation distribution. For conciseness, the respective EBSD maps are not shown in this paper but an example is available as supplementary data (Fig. S1a).

After annealing at 300 C (0.46 T_m), the grain structure (Fig. 2b) was noticeably-different relative to that for the as-rolled condition. The principal features comprised a number of nearly-equiaxed LAB free grains within the original heavily-deformed matrix, i.e., the microstructure had become essentially bimodal. The very large difference between the microstructure constituents suggested that the material had undergone the initial stages of recrystallization. In addition, the recrystallized grains often contained annealing twins as well; annealing twins are frequently associated with grain boundary migration. These observations suggest that microstructure development during annealing involved nucleation and growth of strain-free grains followed by grain growth. The growth of the recrystallized grains partially eliminated LABs and substantially increased the proportion of Σ3 (twin) boundaries (Fig. 3a).

From a comparison of Fig. 2a and b, it was deduced that the ultrafine-grain areas developed during cryo-rolling disappeared first during subsequent annealing. By contrast, the coarse remnants of the original grains exhibited relatively-high stability against recrystallization. It was also found that the recrystallized material contained domains with distinctly-different grain sizes (Fig. 2b). These effects are thought to be attributable to the noticeably inhomogeneous distribution of stored work following cryo-rolling (Fig. 2a). Specifically, the higher density of defects within shear bands would likely have promoted preferential nucleation of recrystallization and have given rise to smaller recrystallized grains.

The cryo-rolled material annealed at 400 C (0.55 T_m) revealed a nearly-completely-recrystallized grain structure (Fig. 2c). This behavior led to a markedly-lower proportion of LABs (~10 pct.) and a large fraction of Σ3 annealing-twin boundaries (~50 pct.), as shown in Fig. 3a. However, the overall microstructure was still inhomogeneous, comprising both relatively small (~0.5 mm) and large (>5 μm) grains (Fig. 2c). This

non-uniformity likely resulted from differences in the recrystallization kinetics for the fine- and coarse-grain constituents of the cryo-rolled material seen in Fig. 2a. Nevertheless, the mean grain size (including twin boundaries) was rather fine, i.e., ~0.8 μm (Fig. 3b), thus lying within the ultrafine-grain regime. Hence, cryogenic rolling coupled with low temperature recrystallization annealing may be used to produce an ultrafine-grain structure with only moderate non-uniformity.

For an annealing temperatures of 500 C (0.63 T_m) and higher, the grain structure began to coarsen noticeably (Fig. 3b). Grain growth was greatly enhanced at 900 C (0.95 T_m) with the mean grain size increasing approximately sixfold relative to that developed at 800 C (Fig. 3b). Some grains even achieved a size of the order of a millimeter (Fig. 2d). On the other hand, the microstructural inhomogeneity found in the as-recrystallized condition was gradually smoothed with increasing temperature (e.g., Fig. 2c vs d). However, the proportions of LABs and Σ3 twin boundaries did not change significantly with temperature in the range of 500-900 C (Fig. 3a).

3.2. Crystallographic texture

Orientation distribution functions (ODFs) derived from large EBSD maps provided insight into texture evolution. These maps were based on orientation measurements for ~10,000 to 60,000 grains, including twins. The sole exception was the material annealed at 900 C; due to the coarse-grain nature of the microstructure in this instance (Fig. 2d), the dataset comprised only 1099 grains.

An ODF for the typical ideal texture components developed during rolling of face-centered-cubic metals is presented in Fig. 4a. This ODF can be compared to that for the material in the as-cryorolled condition (Fig. 4b) as well as after subsequent annealing at various temperatures (Fig. 4c-e); for simplicity, only φ2 = 0 and φ2 = 45 sections are shown in the measured ODFs. From these measurements, the peak ODF intensity and development of selected important texture components were determined (Fig. 5).

The cryo-rolled material was characterized by a relatively strong texture (Fig. 5a) which could be described in terms of the superposition of two partial fibers: α< 110>//ND and γ< 111>//ND (Figs. 4b and 5b). The α fiber was more pronounced than the γ fiber (Fig. 5b). Within the α-fiber, strong Brass {110}<112> and Goss {110}<100> components were noted, whereas the γ-fiber was dominated by the Y {111}<112> texture component (Fig. 4b). As shown in previous work [8,9], the Brass and Goss orientations were mainly found in coarse-grain remnants, whereas the γ-fiber and Y component originated from the ultrafine-grain domains of the cryo-rolled microstructure.

After annealing at 100 C (0.3 T_m) and 200 C (0.38 T_m), no fundamental changes in texture were found. For brevity, the ODFs for these annealing temperatures are not shown but an example is available as supplementary data (Fig. S1b). Partial recrystallization at 300 C (0.46 T_m) significantly enlarged the orientation spread (Fig. 4c) and thus weakened the strength of the overall texture (Fig. 5a). The intensities of the α-fiber (Fig. 5b) as well as the Brass and Goss components (Fig. 5c) were reduced. Moreover, the γ-fiber (Fig. 5b) and the Y orientation (Fig. 5c) disappeared almost completely. The latter effect mirrored the disappearance of the heavily-deformed ultrafine-grain domains (Fig. 2b), thus confirming that these areas

were preferential sites for recrystallization. On the other hand, a new recrystallization-induced orientation near the Copper (90; 30; 45) component was found (arrow in Fig. 4c). This orientation was relatively close to the Brass-R (80; 31; 35) texture component which is often observed during recrystallization of Cu-30Zn brass [12].

After completion of the recrystallization process at 400 C (0.55 T_m), the texture became very diffuse (Fig. 4d) and weak (Fig. 5a). Accordingly, the volume fractions of the dominant α-fiber (Fig. 5b) as well as the Brass and Goss components (Fig. 5c) were further reduced. In part, these effects are thought to be related to the extensive formation of annealing twins during recrystallization and grain growth (Figs. 2c and 3a). On the other hand, the recrystallization-induced near-Copper component was measurably strengthened (Fig. 4d), and its volume fraction reached ~10 pct. (Fig. 5c).

In the temperature range of 500-800 C (0.63-0.87 T_m), the texture was found to be stable and showed no significant changes in morphology (Fig. 4e), strength (Fig. 5a), or volume fractions of the principal components (Fig. 5b and c). Subtle texture sharpening observed at 900 C (Fig. 5a) may have been a result of the limited number of grains for the measurements at this temperature.

4. Discussion

Based on the experimental observations summarized in Section 3, four temperature regimes of microhardness, microstructure, and texture evolution during annealing of cryo-rolled Cu-30Zn brass may be defined, viz., T~100-200 C (0.30-0.38 T_m), T~300-400 C (0.46-0.55 T_m), T ~500-800 C (0.63-0.87 T_m), and T ~900 C (0.95 T_m). In each case, the details of the microstructure-evolution process could be further elucidated by isothermal annealing experiments. Nevertheless, some important aspects of the pertinent metallurgical processes can be deduced from the present work, and are briefly discussed below.

Heat treatment at 100 C and 200 C resulted in no significant changes in grain structure and texture but provided measurable strengthening (Fig. 1). Such behavior is usually indicative of an aging process. Prior work in the literature has shown that annealing of cold-worked Cu-30Zn brass in this temperature range may lead to a reduction of lattice parameter [13] and an increase in electrical resistivity [14], both of which are sometimes attributed to solute clustering at stacking faults, i.e., the Suzuki effect [14].

In the temperature range of 300-400 C, the material hardness decreased rapidly (Fig. 1), and microstructure evolution was dominated by recrystallization accompanied by the formation of annealing twins (Fig. 2b). This process led to a substantial reduction in the fraction of LABs, a significant increase in the proportion of Σ3 twin boundaries (Fig. 3a), and marked changes in texture (Figs. 4 and 5). Although some details are not clear, the recrystallization was probably discontinuous in nature and occurred somewhat differently in the two principal constituents of the cryo-rolled microstructure: the ultrafine-grain domains and the coarse-grain remnants of the original grains. Despite such nonuniformity, the overall recrystallized microstructure was still ultrafine on average with a mean grain size of ~0.8 μm, HAB fraction of ~90 pct., and a weak texture. The strength of this recrystallized material was only ~30 pct. lower than that in the as-cryo-rolled condition (Fig. 1).

An increase in the annealing temperature to 500-900 C gave rise to substantial microstructural coarsening (Fig. 3b), but led to no significant changes in grain morphology, misorientation distribution (Fig. 3a), or texture (Figs. 4 and 5). This suggests that microstructure evolution was governed by normal grain growth.

In this temperature range, vaporization of Zn from brass is known to occur [e.g. Ref. [15]]; this process should become particularly pronounced at ~900 C [16]. This phenomenon might contribute to diffusion-assisted processes in the material [17]. It is possible therefore, the observed abrupt grain growth at 900 C (Fig. 3b) was related with the dezincification effect; this assumption warrants experimental verification, however.

Remarkably, despite the pronounced grain coarsening in the 800-900 C temperature range (Fig. 3b), there was no significant reduction in hardness (Fig. 1). This observation may indicate that the mean free slip length did not exceed ~20 μm, i.e., a length substantially less than the grain size per se.

5. Summary

The annealing behavior of cryogenically-rolled Cu-30Zn brass was investigated. For this purpose, the material was rolled to a 90pct. thickness reduction at liquid-nitrogen temperature and then isochronally annealed at temperatures between 100 C (0.30 T_m) and 900 C (0.95 T_m) for 1 h. Grain-structure and texture changes were followed using an EBSD technique. The main conclusions from this work are as follows:

In the temperature range of 100-200 C (0.30-0.38 T_m), microstructure changes appeared to be governed by solute clustering at stacking faults, i.e., the Suzuki effect. At 300-400 C (0.46-0.55 T_m), discontinuous recrystallization became the dominant mechanism. This process fundamentally altered the grain structure, misorientation distribution, and crystallographic texture. For an annealing temperature of 500 C (0.63 T_m) and higher, microstructure evolution was interpreted in terms of normal grain growth which provided significant changes neither in misorientation distribution nor texture. Grain coarsening was significantly enhanced at 900 C (0.95 T_m).

The recrystallizated microstructure developed at 400 C (0.55 Tm) was within the ultrafine-grain range and was characterized by a mean grain size of 0.8 μm, HAB fraction of ~90 pct., and a weak texture. The strength of the recrystallized material was only ~30 pct. lower than that in the as-cryo-rolled condition.

Acknowledgments

Financial support from the Russian Fund for Fundamental Research (project No.14-02-97004) is gratefully acknowledged. The authors are grateful to P. Klassman for technical assistance during cryogenic rolling.

References

[1] Y. Huang, P.B. Prangnell, The effect of cryogenic temperature and change in deformation mode on the limiting grain size in a severely deformed dilute aluminum alloy, Acta Mater. 56 (2008) 1619-1632.

[2] T. Konkova, S. Mironov, A. Korznikov, S.L. Semiatin, Microstructural response of pure copper to cryogenic rolling, Acta Mater 58 (2010) 5262-5273.

[3] S.V. Zherebtsov, G.S. Dyakonov, A.A. Salem, V.I. Sokolenko, G.A. Salishchev, S.L. Semiatin, Formation of nanostructures in commercial-purity titanium via cryo-rolling, Acta Mater. 61 (2013) 1167-1178.
[4] G.H. Xiao, N.R. Tao, K. Lu, Microstructures and mechanical properties of a CuZn alloy subjected to cryogenic dynamic plastic deformation, Mater. Sci. Eng. A 513-514 (2009) 13-21.
[5] Y.S. Li, N.R. Tao, K. Lu, Microstructural evolution and nanostructure formation in copper during dynamic plastic deformation at cryogenic temperatures, Acta Mater. 56 (2008) 230-241.
[6] Y. Zhang, N.R. Tao, K. Lu, Mechanical properties and rolling behaviors of nanograined copper with embedded nano-twin bundles, Acta Mater. 56 (2008) 2429-2440.
[7] J. Das, Evolution of nanostructure in a-brass upon cryo-rolling, Mater. Sci. Eng. A 530 (2011) 675-679.
[8] T. Konkova, S. Mironov, A.V. Korznikov, G. Korznikova, M.M. Myshlyaev, S.L. Semiatin, Grain structure evolution during cryogenic rolling of alpha brass, J. Alloys Compd. 629 (2015) 140-147.
[9] T. Konkova, S. Mironov, A.V. Korznikov, G. Korznikova, M.M. Myshlyaev, S.L. Semiatin, An EBSD investigation of cryogenically-rolled Cu-30%Zn brass, Mater. Character 101 (2015) 173-179.
[10] J. Hirsch, K. Lucke, M. Hatherly, Mechanism of deformation and development of rolling textures in polycrystalline F.C.C. metals: III. The influence of slip inhomogeneities and twinning, Acta Metall. 36 (1988) 2905-2927.
[11] F.J. Humphreys, Quantitative metallography by electron backscatter diffraction, J. Microsc. 195 (1999) 170-185.
[12] F.J. Humphreys, M. Hatherly, Recrystallization and Related Phenomena, second ed., Elsevier, Oxford, 2000.
[13] H.M. Otte, Lattice parameter studies of annealed, of aged, and of cold-worked alpha brass, J. Appl. Phys. 33 (6) (1962) 1436-1441.
[14] H.I. Fusfeld, Effect of cold work on resistivity of alpha brass, J. Appl. Phys. 24 (1953) 1062-1063.
[15] F.W. Giacobbe, Thermodynamic dezincification behavior of brass during annealing, J. Alloys. Comp. 202 (1993) 243-250.
[16] J.-M. Koo, H. Araki, S.-B. Jung, Effect of Zn addition on mechanical properties of brass hollow spheres, Mater. Sci. Eng. A 483e484 (2008) 245-257.
[17] V.Y. Doo, R.W. Balluffi, Structural changes in single crystal copper-alpha brass diffusion couples, Acta Metall. 6 (1958) 428-438.

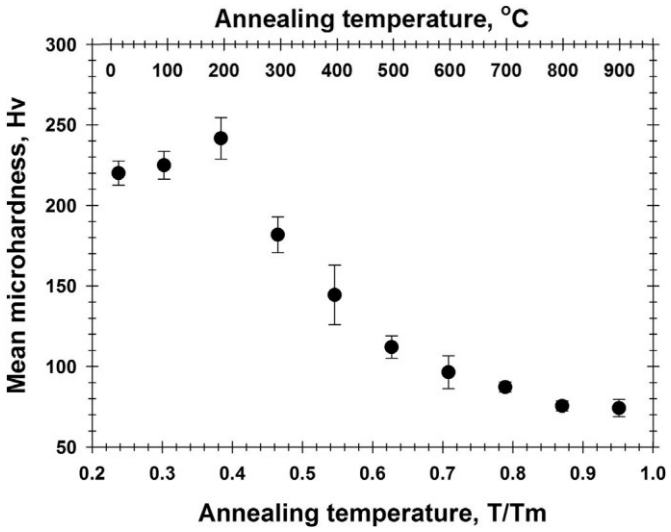

Fig. 1. Effect of annealing temperature on microhardness. Error bars show the standard deviation of the measurements.

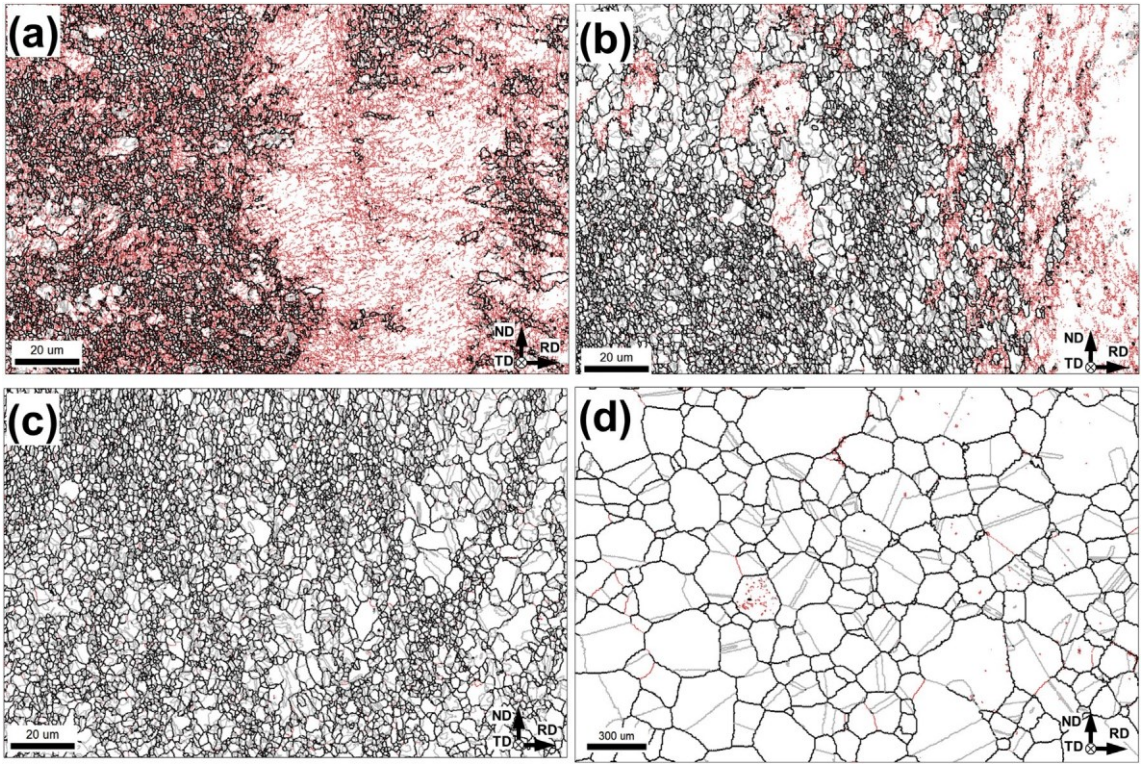

Fig. 2. Selected portions of grain-boundary EBSD maps showing the grain structure which developed (a) after cryo-rolling and subsequent annealing at (b) 300 C (0.46 T_m), (c) 400 C (0.55 T_m), or (d) 900 C (0.95 T_m). In the maps, red, black, and gray lines depict LABs, HABs, and Σ3 twin boundaries (within a 5° tolerance), respectively; RD, ND and TD denote the rolling, normal, and transverse directions, respectively. Note the different magnifications. (For interpretation of the references to colour in this figure legend, the reader is referred to the web version of this article.)

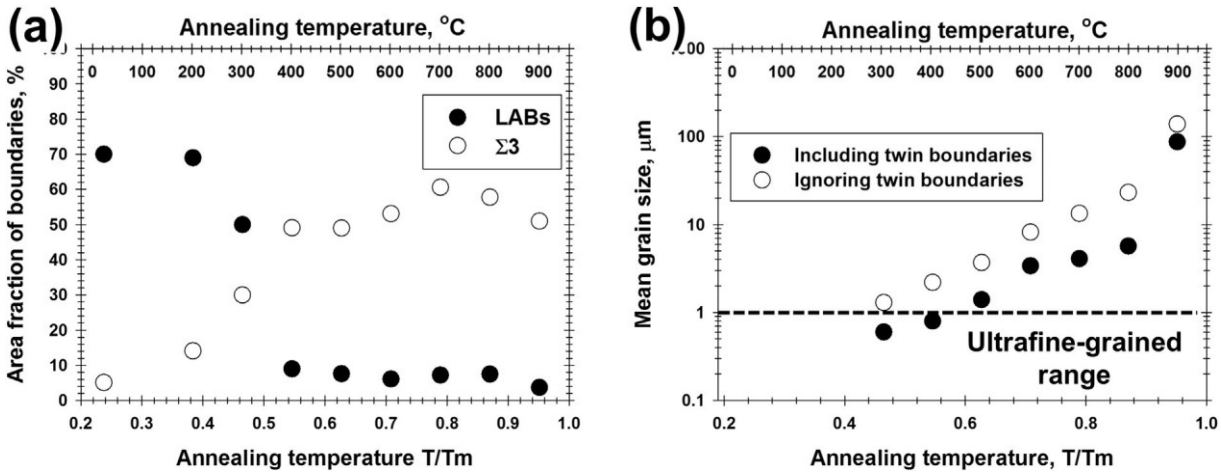

Fig. 3. Effect of annealing temperature on (a) the area fraction of LABs and Σ3 twin boundaries and (b) the mean size of recrystallized grains. In (a), the fraction of Σ3 twin boundaries is based on the Brandon criterion.

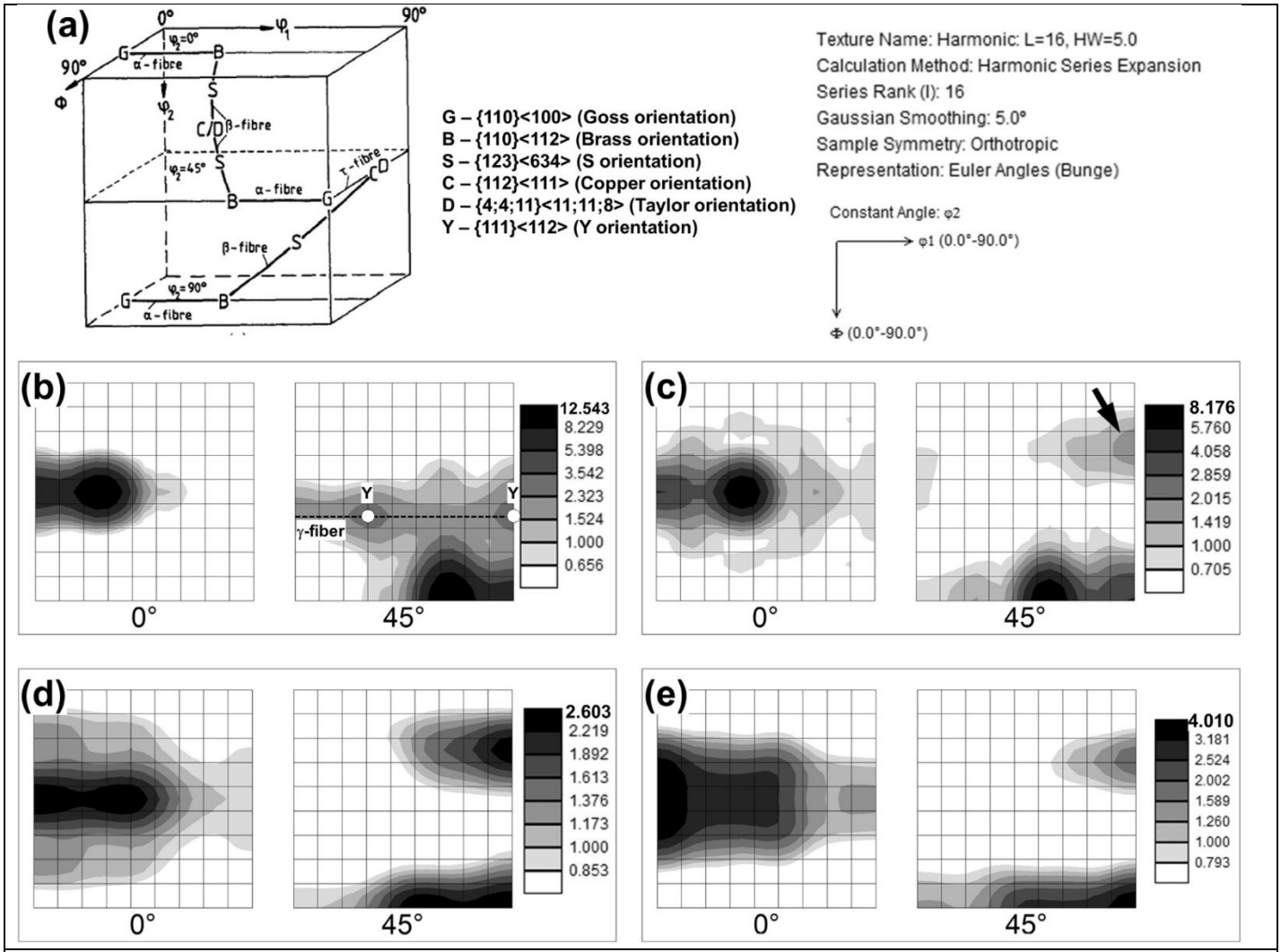

Fig. 4. Orientation distribution functions (ODF) illustrating (a) ideal rolling texture components for fcc metals, and the textures developed (b) during cryogenic rolling, or cryogenic rolling followed by annealing at (c) 300 C (0.46 T_m), (d) 400 C (0.55T_m), or (e) 800 C (0.87 T_m). For simplicity, only φ2 = 0 and φ2 = 45 ODFs' sections are shown in the measured texture.

Effect of annealing temperature on (a) the peak intensity in the ODFs ,and the volume fractions of (b) the main textures and (c) the main texture components. Note: the volume fractions in (b) and (c) were determined based on a 15-deg spread around each ideal component.

Fig.5.